Mixed Convective Flow of Electrically Conducting Fluid in a Vertical Cylindrical Annulus With Moving Walls Adjacent to a Radial Magnetic Field Along With Transpiration

Ali Shakiba
Department of Mechanical Engineering,
Ferdowsi University of Mashhad,
Mashhad 1111, Iran

Asghar B. Rahimi[1]
Professor
Faculty of Engineering,
Ferdowsi University of Mashhad,
P.O. Box 91775-1111,
Mashhad 1111, Iran,
e-mail: rahimiab@yahoo.com

The steady, viscous flow and mixed convection heat transfer of an incompressible electrically conducting fluid within a vertical cylindrical annulus with moving walls are investigated. This annulus is under the influence of a radial magnetic field and the fluid is suctioned/injected through the cylinders' walls. An exact solution of the Navier–Stokes equations and energy equation is derived in this problem where heat is transferred from the hot cylinder walls with constant temperature to the cooler moving fluid. The role of the movement of the annulus walls is studied on the flow and heat transfer of the fluid within the annulus, for the first time. The effects of other parameters, including Prandtl number, Hartman number, mixed convection parameter, suction/injection parameter and ratio of the radius, on the behavior of the flow and heat transfer of the fluid is also considered. The results indicate that if, for example, the internal cylinder wall moves in the direction of z-axis and the external cylinder is stationary, the maximum and minimum heat transfer occur on the walls of internal and external cylinders, respectively. Moreover, the augmentation of the radius ratio between the two cylinders increases the rate of heat transfer and decreases the shear stress on the wall of the internal and external cylinders, however, the results on the wall of external cylinder are exactly the reverse. Consequently, by changing the effective parameters used in this paper, the flow of the fluid can be controlled and the heat transfer of the fluid can be improved.
[DOI: 10.1115/1.4042563]

Keywords: mixed convection, vertical annulus, moving walls, transpiration, magneto-hydrodynamics

1 Introduction

In recent years, increasing the efficiency and reducing the size of heat transfer instruments have always been of interest to the researchers. It is worth mentioning here that different methods, such as the use of fins, suction/injection and vibration of heated surfaces in the flow of the fluids, were used to adjust the rate of heat transfer. In this regard, its effects on the flow of the fluids was explored in the form of boundary conditions, different geometries as well as various solving methods. The mixed convection heat transfer has always attracted the attention of the researchers due to its applications in the cooling of electronic components, food industry, heat exchangers, metal melting industry, solar collectors and so on [1]. Thus, the problem of heat transfer in vertical cylindrical annulus with suction/injection, containing an electrically conducting fluid exposed to the radial magnetic field, is of great importance. Iannello et al. [2] gained analytical solutions for vertical flow and mixed convection heat transfer within annular and conventional rod bundle subchannel geometries.

The flow was assumed fully developed and in laminar regime. The results of their research represented the correlation of Nusselt number and friction coefficient on the wall with the mixed convection parameter. Barletta [3] studied mixed convection of laminar and fully developed power-law fluid flow in a vertical annular duct analytically. He solved governing equations and attained results for the velocity, viscous stress and temperature fields. The obtained velocity profile represented the reverse flow in the specified values of the mixed convection parameter. It was reported that the values of this parameter are dependent on the ratio of the radius of the annulus. Avci and Aydın [4] performed an investigation on mixed convection flow in a vertical micro-annulus produced by two concentric micro tubes. By considering fully developed flow, they indicated that increasing the mixed convection parameter intensifies heat transfer as rarefaction effects considered by the velocity slip and temperature jump in the slip flow regime diminish it. Jha et al. [5] investigated the combined effects of suction/injection and wall surface curvature on natural convection flow in a vertical annular microchannel. They discovered that for the internal cylinder, in case of injection at internal cylinder and simultaneously suction at external cylinder with growth of fluid-wall interaction parameter, skin-friction declines while the result was just opposite at the external cylinder.

Magneto-hydrodynamics (MHD) occurs when electrically conducting fluid is affected by the magnetic field. Lorentz force is

[1]Corresponding author.

Contributed by the Fluids Engineering Division of ASME for publication in the Journal of Fluids Engineering. Manuscript received October 11, 2018; final manuscript received January 17, 2019; published online March 4, 2019. Assoc. Editor: Nazmul Islam.

one of the most important phenomena that arise in such matters. The flow of fluid which is influenced by the magnetic field is used for the purpose of cooling electronic systems, electrical transformers, biochemical and physical phenomena such as geological phenomena, atmospheric flows, and the like [6]. For example, the presence of convection flows in casting industry leads to the emergence of a heterogeneous in the casting piece. It is notable that the amount of these convection flows can be reduced with the help of magneto-hydrodynamics. However, in some related problems in which the cooling of the fluid is intended the operating fluid may inadvertently and forcedly be affected by the magnetic field and thus results in reducing the value of heat transfer which is not indeed desirable. Therefore, in these cases, the researchers are looking for some strategies to increase the amount of heat transfer for rectifying the depletion effect of magnetic field. An example of this phenomenon can occur for an electronic piece that is influenced by a magnetic field and cooled by a fluid. Singh et al. [7] examined natural convection in vertical concentric annuli. They considered that the fluid flow is fully developed and annuli exposed to radial magnetic field. They solved governing equations exactly and concluded that Hartmann number lessened both skin-friction and mass flow rate. Jha et al. [8] studied magneto-hydrodynamic natural convection flow in a vertical microchannel. They considered suction/injection on the walls of microchannel and found out that as suction/injection, rarefaction and fluid-wall interaction enhance, the volume flow rate increased while it diminished with the increase of Hartmann number.

Freidoonimehr and Rahimi [9] conducted an exact solution for nanofluid flow and heat transfer and also entropy generation analysis. They considered that fluid flow is in the steady-state and laminar regime and it exposed to a magnetic field. Their results revealed that averaged entropy generation number for both copper and aluminum oxide nanoparticles is the largest and the lowest, respectively.

Jha and Aina [10] analyzed MHD natural convection flow of electrically conducting fluid in a vertical cylindrical annulus microchannel in the presence of imposed radial magnetic field. They found out that in a constant Hartmann number, the skin friction profiles in the presence of induced magnetic field were higher compared to the case when the induced magnetic field was overlooked.

Investigating the annulus wall movement and its effects on flow and heat transfer, is applicable in the processes of construction and cooling of thermal equipment, such as extrusion and drawing process in manufacturing, polymer coating inside a tube, simulation of a train passing a long tunnel, cooling process like hot rolling, nuclear reactors and nuclear fuel channels [11–13]. Shigechi and Lee [14] surveyed the flow and heat transfer behavior of annuli with moving wall. Considering laminar and fully developed flow, they concluded that with increasing the velocity of the moving wall, skin friction decreases and the changes in the Nusselt number forcefully depend on the thermal boundary conditions. Kim [15] examined the unsteady laminar flow of an electrically conducting fluid in a vertical porous moving plate. The results revealed that in a given magnetic field increasing the values of the suction parameter causes a slight increase in the skin friction coefficient. It was also observed that in different values of the Prandle number, as the suction parameter increases, the heat transfer decreases. Chamkha [16] analytically investigated the flow and heat transfer of a vertical moving plate in the presence of a magnetic field. The results showed that with increasing heat absorption coefficient, Nusselt number and skin friction coefficient decrease. Other researches related to the annulus geometry are available and details can be found in existing literatures [17–25].

Here, the problem of magneto-hydrodynamic flow and heat transfer of an electrically conductive, viscous, incompressible fluid inside an annulus is considered in a complete range of moving walls. Effect of this movement of the walls is examined on the behavior of the flow and heat transfer of the fluid for the first time, along with the effect of other parameters including Prandtl number, Hartman number, mixed convection parameter, suction/injection parameter and ratio of the radius. The results indicate that by changing the effective parameters used in this paper, the flow of the fluid can be controlled and the heat transfer of the fluid can be improved.

In the remaining the problem statement, governing equations, boundary conditions and credibility, results and discussions, and conclusions will be presented.

2 Problem Statement

Mixed convection flow within a vertical cylindrical annulus containing an electrically conducting fluid is studied by considering the effects of suction/injection and radial magnetic field. The image of the geometry related to the annulus which contains an electrically conductive fluid along with its boundary conditions is shown in Fig. 1. The z-coordinate is considered along the annulus axis and the r-coordinate is perpendicular to it. The radius of the internal and external cylinders is a, and b, respectively, and the surface temperatures of the internal and external cylinders are, respectively, equal to T_1 and T_o ($T_1 > T_o$). Since the length of the annulus is infinity, all physical parameters are function of r, except for the pressure gradient that is function of z. It is assumed that the fluid is suctioned/injected from the walls of the annulus and a magnetic field is applied on it radially with a size equal to B_0a/r. The mixed convective flow of the fluid is investigated in various states, when the internal and external cylinders or both move in the selected directions with constant velocities equal to Au_0 and Bu_0, respectively, and for different values of A, and B.

3 Governing Equations, Boundary Conditions, and Credibility

The fluid is considered laminar, steady, Newtonian, incompressible and fully developed. By applying no-slip condition to the

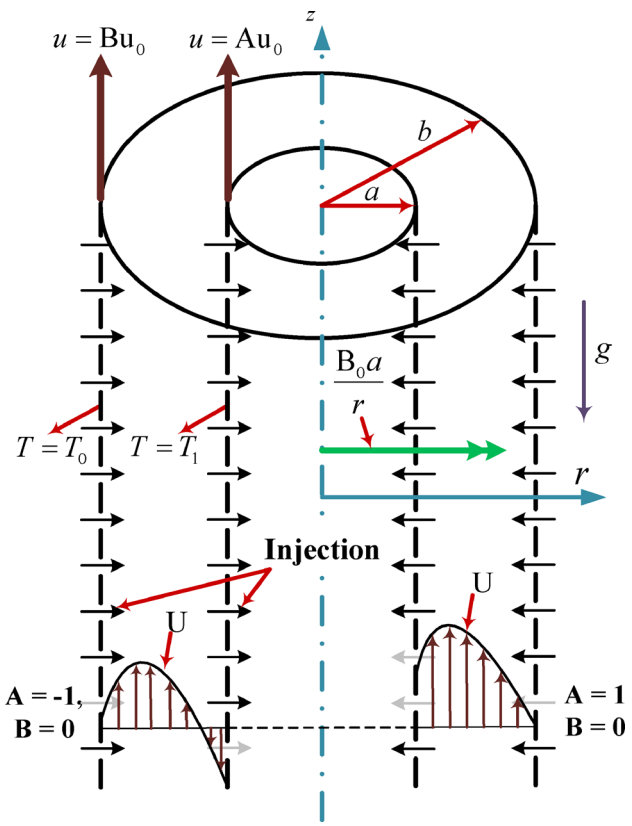

Fig. 1 Geometry and coordinate system of the annulus

walls and by using the Boussinesq approximation, conservation equations including continuity, momentum and energy, are expressed as Eqs. (1)–(3). A key point to note here is that in writing these equations, the axial conduction of the fluid and walls as well as the viscous dissipation and the effects of compressibility are neglected.

Continuity equation

$$\frac{1}{r}\frac{d}{dr}(rV) = 0 \tag{1}$$

Momentum equation

$$V\frac{du}{dr} = -\frac{1}{\rho}\frac{dp}{dz} + \frac{\nu}{r}\frac{d}{dr}\left(r\frac{du}{dr}\right) + g\beta(T - T_0) - \frac{\sigma B^2 u}{\rho} \tag{2}$$

Energy equation

$$\frac{k}{r}\frac{d}{dr}\left(r\frac{dT}{dr}\right) = (\rho C_p)V\frac{dT}{dr} \tag{3}$$

Here, ρ, C_p, σ, and β are density, specific heat, electrical conductivity, and thermal expansion coefficient of the fluid, respectively.

The boundary conditions are as follows:

$$\begin{aligned} &T = T_1, \quad u = Au_o, \quad r = a \\ &T = T_o, \quad u = Bu_o, \quad r = b \end{aligned} \tag{4}$$

In which A and B are constant. It is noted that if both of these constants are equal to zero, then a stationary state for the annulus is indicated. The following nondimensional quantities are introduced:

$$\begin{aligned} &\mathrm{R} = \frac{r}{a}, \quad \lambda = \frac{b}{a}, \quad \theta = \frac{T - T_0}{T_1 - T_0}, \quad Z = \frac{z}{\mathrm{Re}.D_h}, \\ &\mathrm{U} = \frac{u}{u_0}, \quad \mathrm{P} = \frac{p}{\rho u_0^2}, \quad \mathrm{S} = \frac{V_0 a}{\nu}, \quad B = \frac{B_0 a}{r}, \\ &\mathrm{Gr} = \frac{g\beta\Delta T D_h^3}{\nu^2}, \quad \mathrm{Pr} = \frac{\nu}{\alpha_T}, \quad \mathrm{Re} = \frac{u_0 D_h}{\nu}, \\ &\eta = \frac{\mathrm{Gr}}{\mathrm{Re}}, \quad \mathrm{Ha} = B\,D_h\sqrt{\frac{\sigma}{\mu}} \end{aligned} \tag{5}$$

Substituting these nondimensional quantities in the momentum and energy equations and integrating Eq. (1), the following results are obtained:

$$V = \frac{-aV_0}{r} \tag{6}$$

Momentum equation

$$\begin{aligned} &-\frac{S}{R}\frac{d}{dR}U(R) - \frac{1}{R}\frac{d}{dR}\left(R\frac{d}{dR}U(R)\right) \\ &\quad + \frac{1}{4(\lambda-1)^2}\left[\frac{dP}{dZ} + \frac{\mathrm{Ha}^2}{R^2}U(R) - \eta\,\theta(R)\right] = 0 \end{aligned} \tag{7}$$

Energy equation

$$\frac{1}{\mathrm{Pr}}\frac{d}{dR}\left(R\frac{d}{dR}\theta(R)\right) + S\frac{d}{dR}\theta(R) = 0 \tag{8}$$

Relation (6) gives the velocity component in r direction and the nondimensional boundary conditions would be

$$\begin{aligned} &\theta = 1, \quad U = A, \quad R = 1, \\ &\theta = 0, \quad U = B, \quad R = \lambda \end{aligned} \tag{9}$$

At any cross section of the annulus, mean velocity is obtained from Eq. (10) which is regarded as the reference velocity (u_o). Besides, dimensionless volumetric flow rate (Q), which is considered constant at any cross section of the annulus, would be obtained from Eq. (11), as

$$u_0 = u_m = \frac{\int_a^b \mathrm{urdr}}{\int_a^b r\mathrm{dr}} \tag{10}$$

$$Q = \int_1^\lambda RU(R)dR = \int_1^\lambda RdR = \frac{1}{2}(\lambda^2 - 1) \tag{11}$$

By employing the boundary conditions in Eq. (9) and integrating Eqs. (7) and (8), the results of exact solution are obtained as Eqs. (12) and (13)

$$\theta(R) = \frac{-1 + \lambda^{\mathrm{Pr.S}} R^{-\mathrm{Pr.S}}}{-1 + \lambda^{\mathrm{Pr.S}}}, \quad S \neq 0 \tag{12}$$

$$U(R) = C_1 R^{\delta_1} + C_2 R^{\delta_2} + \delta_5 R^2 + \delta_6 R^{2-\mathrm{Pr.S}} \tag{13}$$

The dimensionless bulk temperature can be defined as the following equation:

$$\theta_b = \frac{T_b - T_0}{T_1 - T_0} = \frac{\int_1^\lambda RU(R)\theta(R)dR}{\int_1^\lambda RU(R)dR} \tag{14}$$

And the dimensionless shear stress and the Nusselt number on the cylinders' wall are defined as Eqs. (15) and (16)

$$\begin{aligned} &\tau|_{\mathrm{wall}} = \left.\frac{dU}{dR}\right|_{\mathrm{wall}}, \\ &\begin{cases} \tau_1 = C_1\delta_1 + C_2\delta_2 + 2\delta_5 + \delta_6(-\mathrm{Pr.S} + 2) \\ \tau_\lambda = C_1\lambda^{\delta_1 - 1}\delta_1 + C_2\lambda^{\delta_2 - 1}\delta_2 + 2\delta_5\lambda + \delta_6\lambda^{-\mathrm{Pr.S}+1}(-\mathrm{Pr.S} + 2) \end{cases} \end{aligned} \tag{15}$$

$$\begin{aligned} &\mathrm{Nu}|_{R=1} = -2(\lambda - 1)\frac{\left.\frac{d\theta}{dR}\right|_{R=1}}{\theta|_{R=1} - \theta_b} = \mathrm{Nu}_1 = -\frac{\delta_7\lambda^{\mathrm{Pr.S}}}{(-1 + \theta_b)}, \\ &\mathrm{Nu}|_{R=\lambda} = 2(\lambda - 1)\frac{\left.\frac{d\theta}{dR}\right|_{R=\lambda}}{\theta|_{R=\lambda} - \theta_b} = \mathrm{Nu}_\lambda = \frac{\delta_7}{\theta_b\lambda} \end{aligned} \tag{16}$$

In which C_1, C_2, and δ_1–δ_7 are constant coefficients that they are defined as following:

$$\begin{aligned} &\delta_3 = \left(\mathrm{Pr}(\lambda - 1)^2(\mathrm{Pr} - 1)S^2 - 4(\lambda - 1)^2\left(\mathrm{Pr} - \frac{1}{2}\right)S \right. \\ &\qquad \left. - \frac{\mathrm{Ha}^2}{4} + 4\lambda^2 - 8\lambda + 4\right) \\ &\delta_4 = (\lambda - 1)^2 S - \frac{\mathrm{Ha}^2}{8} + 2\lambda^2 - 4\lambda + 2, \quad \delta_5 = \frac{\eta + (\lambda^{\mathrm{Pr.S}} - 1)\frac{dP}{dz}}{8(\lambda^{\mathrm{Pr.S}} - 1)\delta_4} \\ &\delta_6 = \frac{-2\lambda^{\mathrm{Pr.S}}\eta}{8\delta_3(\lambda^{\mathrm{PrS}} - 1)}, \quad \delta_7 = \frac{2(\lambda - 1)\mathrm{Pr.S}}{(-1 + \lambda^{\mathrm{Pr.S}})} \end{aligned} \tag{17}$$

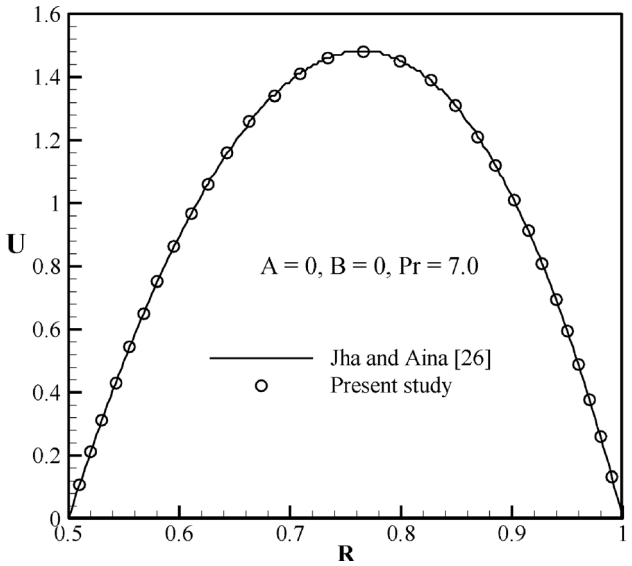

Fig. 2 Comparison of the velocity profile in an annulus with Ref. [26] for $\eta = 50$, $S = -0.5$, $Ha = 0$

$$C_1 = -\frac{\delta_5\lambda^2 + (A - \delta_5 - \delta_6)\lambda^{\delta_2} + \delta_6\lambda^{-\mathrm{Pr}.S+2} - B}{\lambda^{\delta_1} - \lambda^{\delta_2}},$$

$$C_2 = \frac{\delta_5\lambda^2 + (A - \delta_5 - \delta_6)\lambda^{\delta_1} + \delta_6\lambda^{-\mathrm{Pr}.S+2} - B}{\lambda^{\delta_1} - \lambda^{\delta_2}}$$

$$\delta_1 = \frac{S(1-\lambda) - \sqrt{S^2(\lambda-1)^2 + \mathrm{Ha}^2}}{2(\lambda-1)},$$

$$\delta_2 = \frac{S(1-\lambda) + \sqrt{S^2(\lambda-1)^2 + \mathrm{Ha}^2}}{2(\lambda-1)}$$

To demonstrate the exactitude and accuracy of the present study, the obtain results of this study for velocity profile are compared with the work of Jha and Aina [26]. This comparison is performed for the following conditions in this reference as no magnetic field, Knudsen number, Kn = 0, the outer cylinder wall temperature is greater than the inner temperature wall, the cylinder walls are stationary and the Prandtl number and mixed convection parameter are considered equal to 7 and 50, respectively. It is also assumed that the fluid is suctioned on both walls. This comparison is presented in Fig. 2. As it can be seen the consistency between the results is evident.

In Sec. 4, numerical results for some selected values of the parameters involved are presented.

4 Results and Discussion

In this section, some numerical results are presented for selected values of the effect of the motion of cylinders' walls on the flow and heat transfer of electrically conducting and other active parameters, including Hartman number (Ha), Prandtl number (Pr), suction/injection parameter (S), radial ratio (λ), Nusselt number (Nu), and mixed convection parameter (η). As mentioned earlier, we are considering that the direction of heat transfer is from the inner cylinder wall to the fluid, meaning that the inner wall is in higher temperature respected to the fluid and the fluid temperature is initially same as the outer wall temperature.

Also, according to Fig. 1, since the surface of the internal and external cylinders are perforated, $S > 0$ indicates a state that an injection occurs in the cylinders' wall toward the annulus axis and $S < 0$ expresses the inverse of aforesaid state.

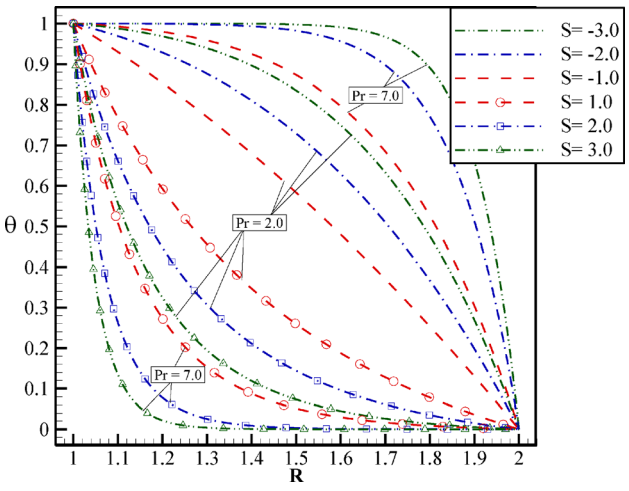

Fig. 3 Dimensionless temperature variations at the interval between two cylinders for different values of suction/injection parameter for upper limit of $R = \lambda = 2$ and two values of $Pr = 2$ and $Pr = 7$

4.1 Temperature Difference Analysis. The dimensionless temperature variations within the annulus for different values of suction/injection parameters in various Prandtl numbers are depicted in Fig. 3. Since the temperatures of internal and external cylinders are higher than the temperature of fluid, the fluid temperature rises due to the heat transfer between the fluid and the walls. If $S > 0$, increase of volume of flow, the temperature of the fluid would decrease against the heated wall of internal cylinder. The value of temperature reduction would also be augmented by increasing S. However, if $S < 0$, the opposite of these results will take place. It is worth mentioning that the increase of Prandtl number reduces the thickness of the thermal boundary layer which means increasing the slope of the dimensionless temperature curve near the wall surface. This effect can be seen comparing the curves related to Pr = 2 and Pr = 7 in Fig. 3.

4.2 Fluid Flow Analysis. The variations of fully developed dimensionless velocity in different states when each of the internal and external cylinders move in the same direction or in the opposite direction of the z-axis is presented here. In Figs. 4(*a*) and 4(*b*), one of the walls is stationary and the other one moves at a constant velocity. In Fig. 4(*c*), both walls move at a uniform velocity. As already mentioned, the volumetric flow rate of the fluid is considered constant at any cross section of the annulus. Therefore, the volumetric flow rate of the fluid decreases when the wall of the cylinder moves in the opposite direction of z-axis and the compensation of its values is accomplished by increasing the pressure difference and the fluid velocity. On the other hand, increasing the values of the wall velocity in the direction of z-axis causes the maximum velocity to decrease and the velocity profile to approach the moving wall. However, the results are just the reverse for the situation in which the wall of the cylinder moves in the opposite direction of z-axis. It is worth noting that the various states of walls' motion and its impact on the dimensionless velocity profile are shown in Fig. 4(*d*). It is evident that when the internal wall moves in the direction of z-axis, the maximum velocity is higher than the situation in which the external wall moves. In fact, this is owing to the presence of the buoyancy force near the heated wall of the internal cylinder.

The variations of the fully developed dimensionless velocity for different values of Hartman numbers are illustrated here. As in Figs. 5(*a*)–5(*c*), the fully developed velocity profiles have a parabolic shape in the absence of a magnetic field and the maximum velocity occurs near the middle of the radial distance between two the cylinders in the annulus. However, by applying radial

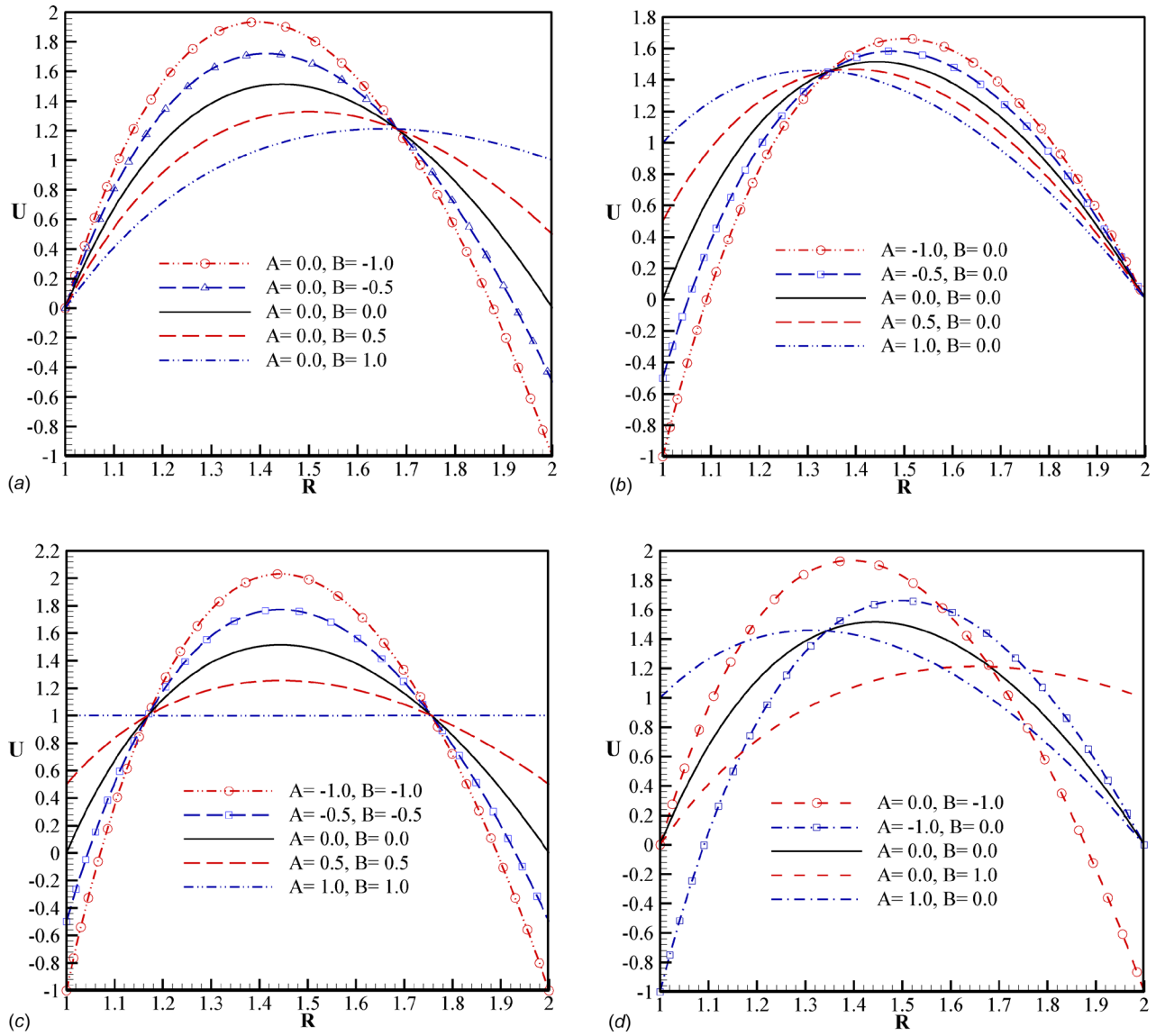

Fig. 4 Effect of the velocity variations of annulus's internal and external cylinders on the dimensionless fully developed velocity profile for $\eta = 5$, $S = 1$, $Pr = 7$, $Ha = 2$, and upper limit of $R = \lambda = 2$

magnetic field, the Lorentz force is exerted axially to the flow of the electrically conducting fluid and as a consequence, the value of the velocity gradient increases near the walls and the velocity profile takes a flat form, meaning that its curvature decreases. Since the radial magnetic field which is applied to the fluid flow has an opposite relation with the radius ($B_0 a/r$), larger Lorentz force is exerted to the fluid near the internal cylinder and its effect will be lessened by approaching the external cylinder.

With regards to Fig. 5(*c*), as the internal cylinder is moving in the absence of a magnetic field, the point in which the maximum velocity occurs will be created adjacent to the heated wall. However, by increasing the intensity of the magnetic field and overcoming the Lorentz force over the buoyancy force and the momentum, the velocity profile takes a flat shape, meaning that its curvature decreases. Hence, for Ha = 20 and Ha = 40 a turning point has been created. Hence, for Ha = 20 and Ha = 40 a turning point has been created. Besides, in Fig. 5(*d*), two extremum points are created due to the movement of both walls and the graph has a turning point. Due to movement of both wall this turning point exist even in the absence of magnetic effect.

In Figs. 6(*a*)–6(*d*), the effect of the variations of transpiration parameter on the dimensionless velocity of the fluid is presented for different states of internal and external cylinders' movement. As it can be seen, the presence of suction/injection on the wall of the internal and external cylinders will lead to velocity variations. In the case of $S > 0$ and compared to no transpiration situation, the extremum points in the velocity profile will move toward the internal wall. In other words, the injection of fluid increases its velocity in the vicinity of the internal cylinder. The opposite of this situation will happen in the case of $S < 0$. In the case of injection, $S > 0$, the velocity in the vicinity of internal wall increases and the volume of fluid in its vicinity also increases. In the case of suction, though, the velocity in the vicinity of the external wall is increased and the volume of fluid in its surrounding increases.

For instance, according to Fig. 6(*d*), if S is equal to zero ($S = 0$), then the maximum point of the velocity happens near the heated wall of the internal cylinder owing to the creation of buoyancy force. Moreover, the minimum point of the velocity occurs in the vicinity of the cold wall of the external cylinder. In this respect, the graph has a turning point.

The effects of the variations of mixed convection parameter (η) on the fully developed dimensionless velocity for different states of internal and external cylinders' movement are illustrated in Figs. 7(*a*)–7(*d*). It is worthy to note that the mixed convection

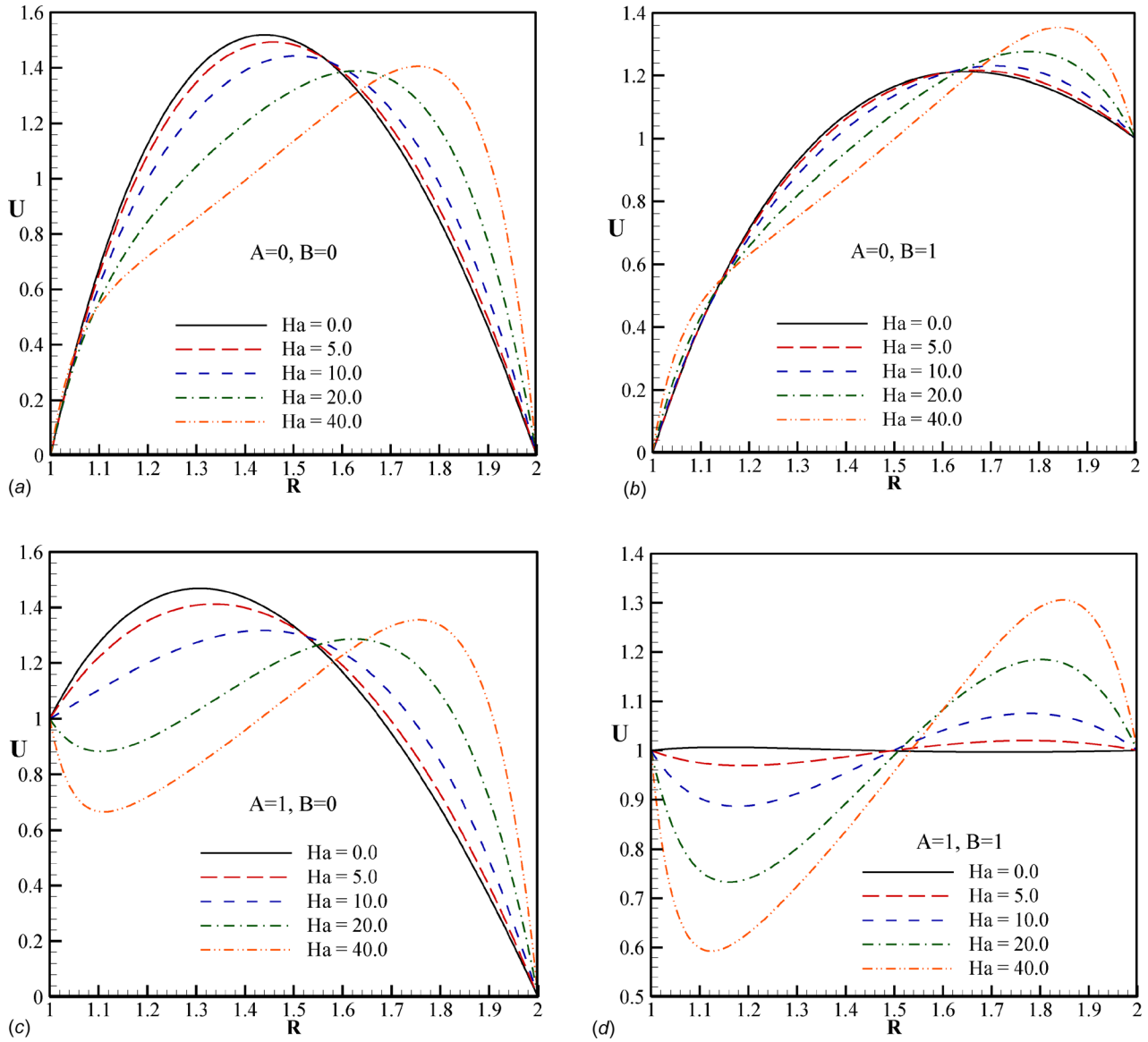

Fig. 5 Variations of fully developed dimensionless velocity for different Hartman numbers and various states of the cylinders' motion for $\eta = 5$, $S = 1$, $Pr = 7$ and upper limit of $R = \lambda = 2$

parameter is a dimensionless number which describes the ratio of the Grashof number to the Reynolds number. As it can be seen, the buoyancy force adjacent to the heated wall is strengthened by increasing η and it will lead to the noticeable increase of fluid velocity against the heated wall. When both walls move together, the fluid has initially more velocity against the cold wall and application of the radial magnetic field and overcoming Lorentz force over buoyancy force is reasoned. However, by increasing η, the buoyancy force gradually dominates the Lorentz force and the fluid velocity increases in the neighborhood of the heated wall.

4.3 Heat Transfer Analysis. The effect of variations of mixed convection parameter on the Nusselt number is given in this section in various states when each of the internal and external cylinders move in the same direction or in the opposite direction of the z-axis. The dimensionless Nusselt number is a parameter which indicates the ratio of convection heat transfer to the conductive heat transfer and it can be calculated on the walls of internal and external cylinders according to Eq. (16). As it can be seen, the buoyancy force is reinforced by enhancing η near the wall of the internal cylinder and it causes, respectively, the increase and decrease of Nusselt number on the walls of internal and external cylinders in different states of internal and external cylinders' movements. As presented in Figs. 8(*a*)–8(*d*), one of the walls is stationary and the other one moves at a constant velocity. The Nusselt number increases and decreases, respectively, on the walls of internal and external cylinders when the velocity of the internal wall gets larger from negative to positive values. The velocity variations in the wall of the external cylinder reveal the inverse of the above results. In Figs. 8(*e*) and 8(*f*), the different states of the motion of cylinders' walls and its effects on the Nusselt number are illustrated. It is worth noting that if the internal cylinder moves in the same direction of z-axis and the external cylinder is stationary, the maximum and minimum heat transfer occur on the walls of the internal and external cylinders, respectively. Moreover, the inverse of these results will be obtained for the Nusselt number if the external cylinder is stationary and the internal cylinder moves in the opposite direction of z-axis.

The impact of increasing the Prandtl number and the changes of radial magnetic field intensity on the Nusselt number are shown in Fig. 9. The dimensionless Prandtl number is a criterion for

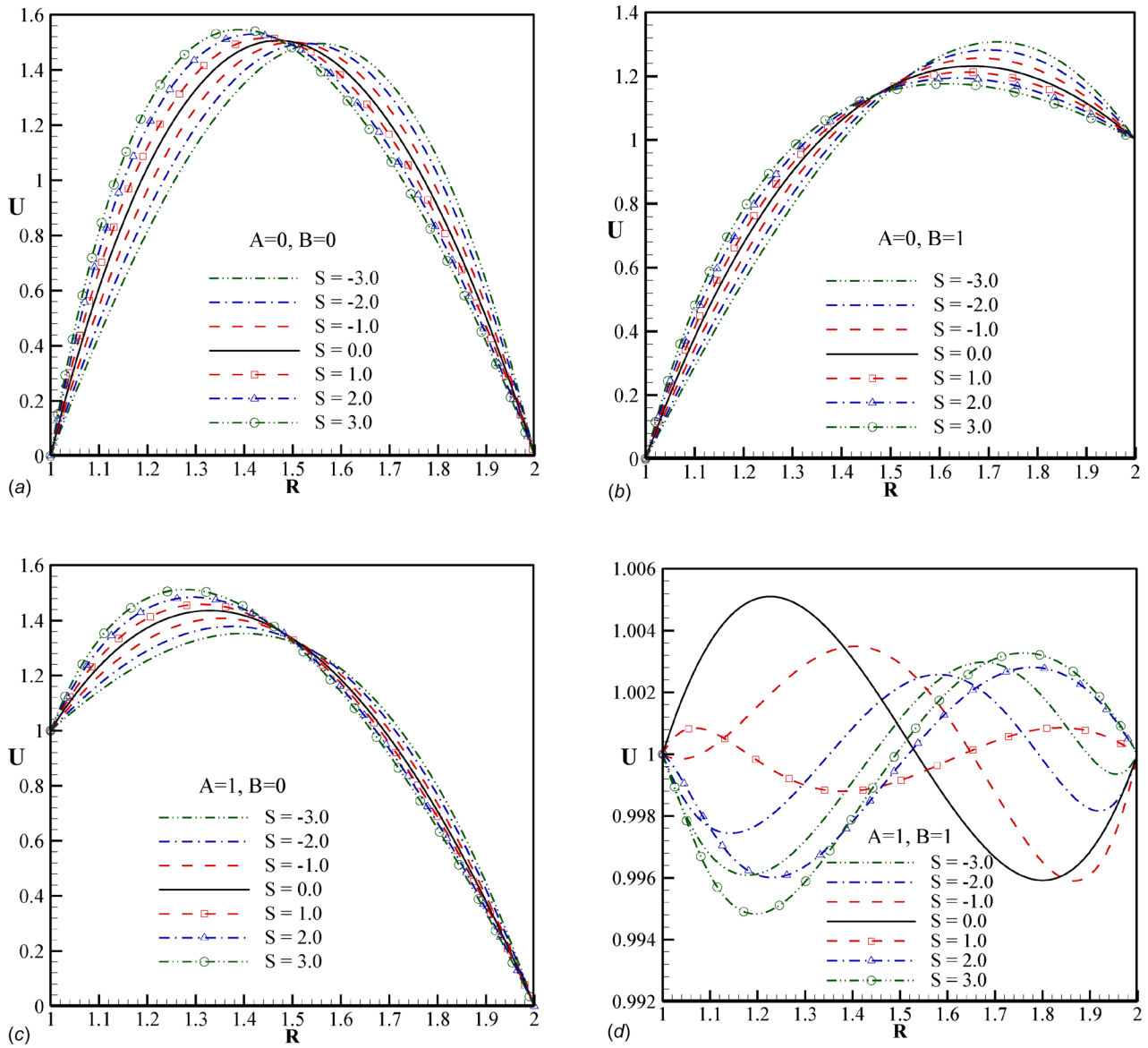

Fig. 6 Variations of S parameter on the dimensionless velocity of fluid for different states of internal and external cylinders' movement for $\eta = 5$, $Pr = 7$, $Ha = 2$ and upper limit of $R = \lambda = 2$

comparing the diffusion of fluid's momentum against the thermal diffusion. Therefore, it is predictable that with the increase of Prandtl number, the thermal diffusion decreases against the diffusion of fluid's momentum and the thickness of the thermal boundary layer diminishes. Consequently, by augmenting the Prandtl number, Nusselt number increases due to the thickness reduction of thermal boundary layer near the internal cylinder's wall. As it can be observed, the fluid temperature decreases near the wall of internal cylinder through increasing the Hartman number and applying the Lorentz force. Besides, by enhancing the temperature difference between the heated wall's temperature and the bulk temperature of the fluid, the fluid is cooled and the Nusselt number decreases. But the Nusselt number on external wall by increases by increasing the Hartman number and decreases by increase of Prandtl number. Note that this is exactly the inverse of what happens on the internal wall.

The graph of the Nusselt number variations on the internal and external cylinders' walls for different radial ratios and various suction/injection parameters are displayed in Fig. 10. According to this figure, with the increase of S parameter, the Nusselt number is approximately constant for the internal cylinder within the limits of $S < 0$ and it increases with a slight slope; however, the Nusselt number gets larger with the increase of S in case of $S > 0$. This is because when $S > 0$ the fluid volume entering the wall increases and therefore the existing boundary layer thickness on the inner wall to decrease which causes abrupt increase in Nusselt number. But when $S < 0$ the changes in boundary layer thickness is not sensible and thus the Nusselt number is almost without change. Note that this trend is the same for all radial ratios. It should be mentioned that by the same argument and for the external wall for $S > 0$ Nusselt number is approximately with no change as S increases and for $S < 0$ Nusselt number increases as S decreases and λ increases.

4.4 Surface Tension Analysis. The effect of increasing mixed convection parameter on the shear stress in different states of internal and external cylinders' movements are illustrated in Fig. 11. Since the shear stress has a direct relation with the velocity gradient, the increase of η reinforces the buoyancy force and the velocity gradient increases near the heated wall of the internal cylinder. Accordingly, the shear stress increases in different states

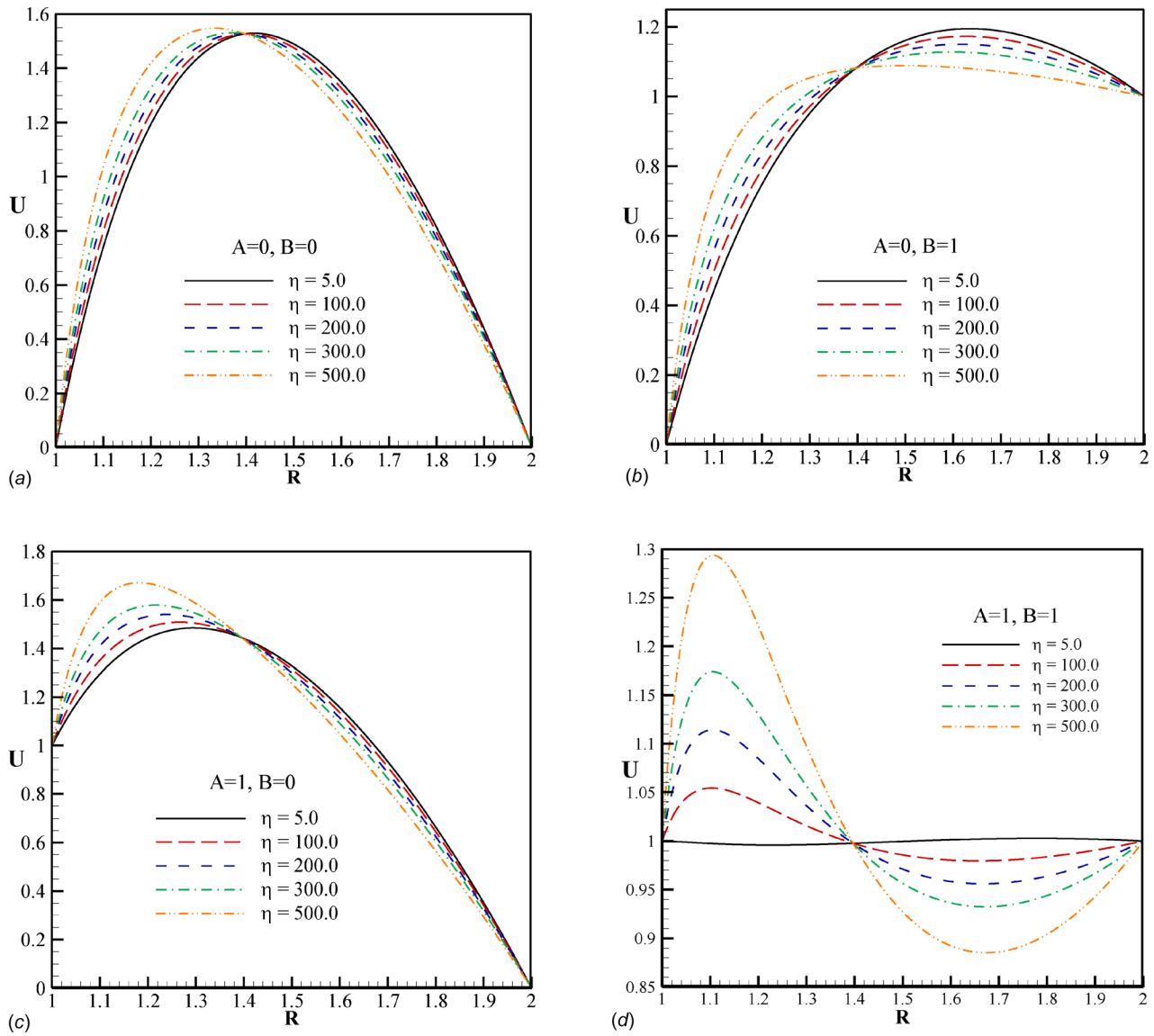

Fig. 7 Effects of the variations of mixed convection parameter on the fully developed dimensionless velocity for different states of internal and external cylinders' movement for $S = 2$, $Pr = 7$, $Ha = 2$, and upper limit of $R = \lambda = 2$

of internal and external cylinders' movement. Thus, as expected, the shear stress is higher than the rest of the states for internal cylinder when two cylinders move in the opposite direction of z-axis and it is the lowest when both the internal and external cylinders move at a constant velocity in the same direction of z-axis. It is notable that the reverse of these results takes place for the shear stress on the external cylinder.

The impacts of the changes of the radial ratio (λ) between two cylinders, Hartman number (Ha) and suction/injection parameter on the shear stress of the fluid are presented in Fig. 12. Regarding this figure, it is evident that in the absence of the magnetic field and with increasing S parameter, the shear stress increases on the wall due to the augmentation of velocity gradient.

Also, in the presence of radial magnetic field, the Lorentz force is the dominant force on the flow and the shear stress decreases with the increase of S parameter. In addition, as it can be seen, the velocity gradient turns to negative and, as a result, the shear stress also becomes negative through applying the magnetic field. In addition, with increasing λ, the velocity gradient decreases in the adjacency of both internal and external cylinder's wall and the shear stress also diminishes.

5 Conclusions

In this paper, an exact solution has been obtained for the mixed convective flow of an electrically conducting fluid in vertical cylindrical annulus in the adjacency of a radial magnetic field. The graphs of the velocity, temperature, shear–stress and Nusselt number have been provided for different values of Hartman number, mixed convection parameter, suction/injection parameter and radial ratio in complete range of states of internal and external cylinders' movement. Following results have been concluded:

- The fluid injection ($S > 0$) increases its velocity in the vicinity of the internal cylinder's wall and the Nusselt number increases on this wall with the enhancement of S.
- Increasing the mixed convection parameter (η) gives rise to the buoyancy force and causes the fluid velocity to increase in the vicinity of internal cylinder's wall. In this regard, the Nusselt number and the shear stress increase on the internal cylinder's wall for different states of internal and external cylinders' movements.

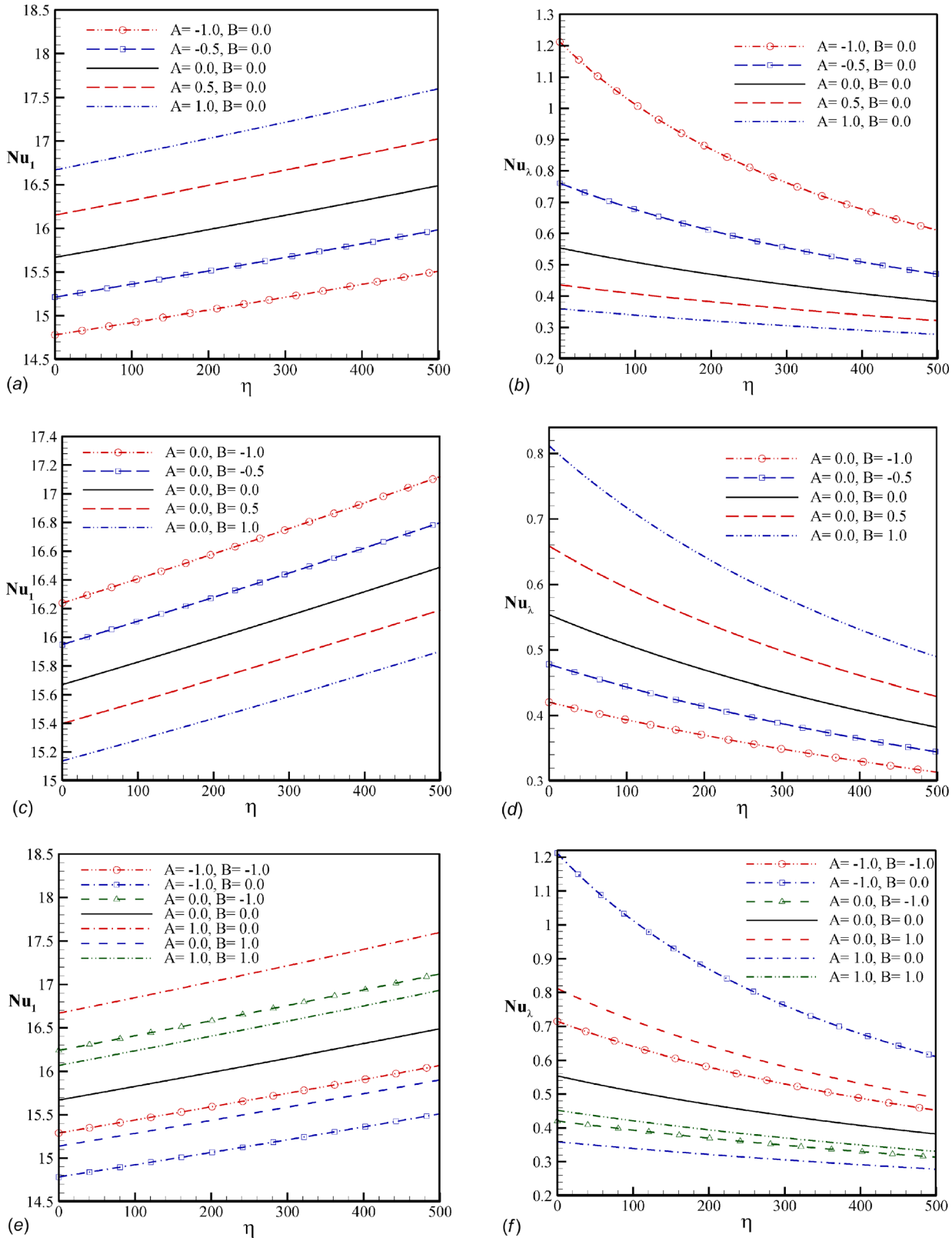

Fig. 8 Effect of the variations of mixed convection parameter on the Nusselt number for different states of internal and external cylinders' movements for $S = 1$, $\lambda = 2$, $Pr = 7$, $Ha = 2$

- If the internal cylinder moves in the same direction of z-axis and the external cylinder is stationary, the maximum and minimum heat transfer occur on the walls of the internal and external cylinders, respectively. Moreover, the inverse of these results will be obtained for the Nusselt number if the external cylinder is stationary and the internal cylinder moves in the opposite direction of z-axis.
- By augmenting the Prandtl number, the Nusselt number increases and decreases, respectively, on the walls of the internal and external cylinders due to the thickness reduction

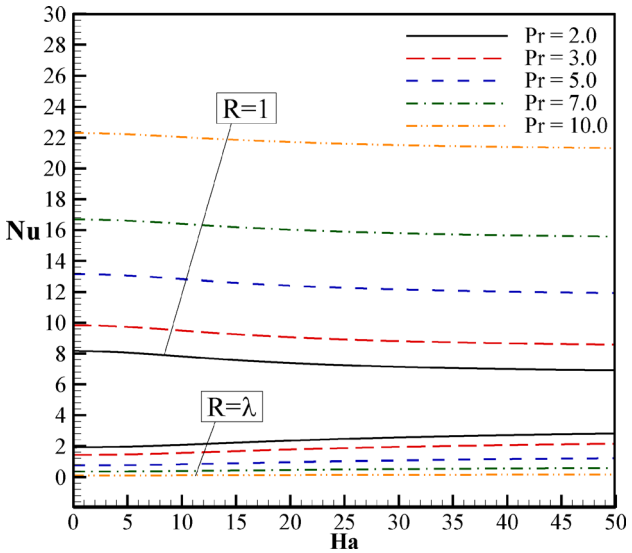

Fig. 9 Impact of dimensionless Prandtl number's changes and the variations of radial magnetic field intensity on the Nusselt number in $A = 1, B = 0, R = 1, \eta = 5, S = 1, \lambda = 2$

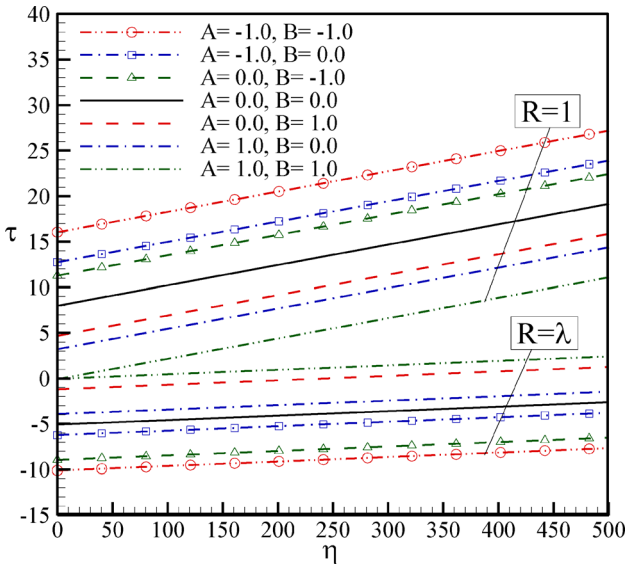

Fig. 11 Variations of shear stress in terms of mixed convection parameter for different states of internal and external cylinders' movements in $Pr = 7$, $Ha = 2$

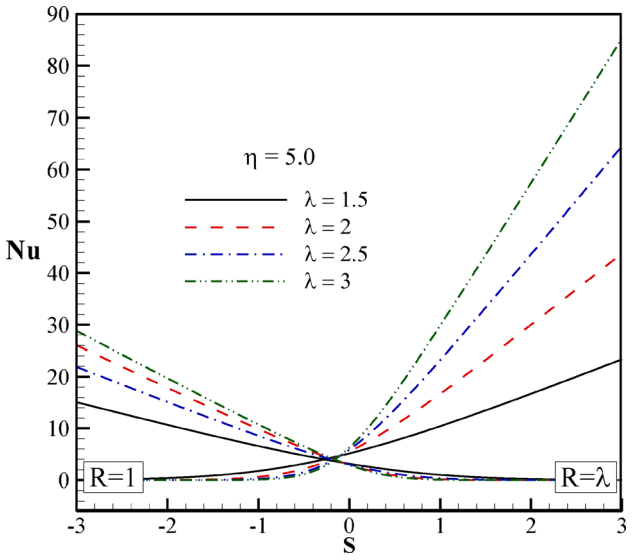

Fig. 10 Variations of Nusselt number for different radial ratios and various suction/injection parameters in $A = 1, B = 0, \eta = 5$, $Pr = 7, Ha = 2$

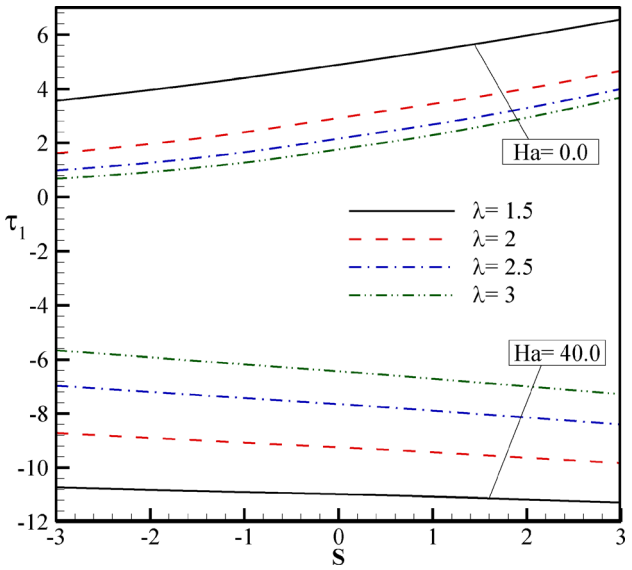

Fig. 12 Variation of radial ratio between two cylinders (λ), Hartman number (Ha) and S parameter on the shear stress of the fluid in $A = 1$, $B = 0$, $\eta = 5$, $Pr = 7$

of the thermal boundary layer near the wall of the internal cylinder.

- By applying radial magnetic field, the Lorentz force is exerted axially to the flow of electrically conducting fluid and it causes the velocity profile to take a flat form.
- In the absence of the magnetic field for the wall of internal cylinder, the shear stress increases with the enhancement of S and on the other hand, the shear stress decreases in the presence of the magnetic field.
- The Nusselt number and the shear stress decrease and increase, respectively, on the wall of internal cylinder through increasing the Hartman number and applying the Lorentz force.
- The increase of λ reduces the shear stress and enhances the Nusselt number on the wall of the internal and external cylinder.

Consequently, the flow and heat transfer rate of fluid in vertical cylindrical annulus can be improved by changing the effective parameters used in this paper.

Nomenclature

a = radius of the inner cylinder (m)
A = coefficient of velocity for inner cylinder
b = radius of the outer cylinder (m)
B = coefficient of velocity for outer cylinder
B_0 = constant magnetic field (T)
C_p = specific heat (J/kg K)
D_h = hydrolic diameter, $D_h = 2(b - a)$
G = gravitational acceleration (m/s^2)
Gr = Grashof number
Ha = Hartman number

K = thermal conductivity (W/m K)
Nu = Nusselt number
P = pressure (Pa)
P = dimensionless pressure
Pr = Prandtl number
Q = dimensionless volumetric flow rate
R = axis in the cylindrical coordinates
Re = Reynolds number
S = suction/injection parameter
T = temperature of fluid (K)
T_0 = wall temperature of outer cylinder (K)
T_1 = wall temperature of inner cylinder (K)
U = velocity in z direction (m/s)
u_m = dimensionless mean velocity
u_0 = reference constant velocity (m^2/s)
V = velocity in r direction (m/s)
Z = axis in the cylindrical coordinates
ΔT = temperature difference, $\Delta T = T_1 - T_0$

Greek Symbols

α_T = thermal diffusivity(m^2/s), $\alpha_T = k/\rho C_p$
β = thermal expansion coefficient (1/K)
η = mixed convection parameter
Θ = dimensionless temperature of fluid
Λ = ratio of the radius between two cylinders
μ = dynamic viscosity (kg/(m/s))
ν = kinematic viscosity (m^2/s), $\nu = \mu/\rho$
ρ = density (kg/m^3)
σ = electrical conductivity ($m^{-1}\Omega^{-1}$)
τ = dimensionless shear stress

Subscripts

b = bulk temperature
m = mean value
λ = value on outer wall
1 = value on inner wall

References

[1] Bhattacharya, M., Basak, T., Oztop, H. F., and Varol, Y., 2013, "Mixed Convection and Role of Multiple Solutions in Lid-Driven Trapezoidal Enclosures," Int. J. Heat Mass Transfer, **63**, pp. 366–388.
[2] Iannello, V., Suh, K. Y., and Todreas, N. E., 1988, "Mixed Convection Friction Factors and Nusselt Numbers in Vertical Annular and Subchannel Geometries," Int. J. Heat Mass Transfer, **31**(10), pp. 2175–2189.
[3] Barletta, A., 2000, "Combined Forced and Free Flow of a Power-Law Fluid in a Vertical Annular Duct," Int. J. Heat Mass Transfer, **43**(19), pp. 3673–3686.
[4] Avcı, M., and Aydın, O., 2009, "Mixed Convection in a Vertical Microannulus Between Two Concentric Microtubes," ASME J. Heat Transfer, **131**(1), p. 014502.
[5] Jha, B. K., Aina, B., and Muhammad, S., 2015, "Combined Effects of Suction/Injection and Wall Surface Curvature on Natural Convection Flow in a Vertical Micro-Porous Annulus," Thermophys. Aeromech., **22**(2), pp. 217–228.
[6] Mahian, O., Mahmud, S., and Pop, I., 2012, "Analysis of First and Second Laws of Thermodynamics Between Two Isothermal Cylinders With Relative Rotation in the Presence of MHD Flow," Int. J. Heat Mass Transfer, **55**(17–18), pp. 4808–4816.
[7] Singh, S., Jha, B., and Singh, A., 1997, "Natural Convection in Vertical Concentric Annuli Under a Radial Magnetic Field," Int. J. Heat Mass Transfer, **32**(5), pp. 399–401.
[8] Jha, B. K., Aina, B., and Ajiya, A., 2015, "Role of Suction/Injection on MHD Natural Convection Flow in a Vertical Microchannel," Int. J. Energy Technol., **7**, pp. 30–39.
[9] Freidoonimehr, N., and Rahimi, A. B., 2017, "Exact-Solution of Entropy Generation for MHD Nanofluid Flow Induced by a Stretching/Shrinking Sheet With Transpiration: Dual Solution," Adv. Powder Technol., **28**(2), pp. 671–685.
[10] Jha, B., and Aina, B., 2018, "Impact of Induced Magnetic Field on Magnetohydrodynamic (MHD) Natural Convection Flow in a Vertical Annular Micro-Channel in the Presence of Radial Magnetic Field," Propul. Power Res., **7**(2), pp. 171–181.
[11] Strafford, K. N., Datta, P. K., and Coogan, C., 1984, *Coatings and Surface Treatment for Corrosion and Wear Resistance*, Ellis Horwood, Chichester, UK, p. 362.
[12] Lin, S., and Hsieh, D., 1980, "Heat Transfer to Generalized Couette Flow of a Non-Newtonian Fluid in Annuli With Moving Inner Cylinder," ASME J. Heat Transfer, **102**(4), pp. 786–789.
[13] Huang, S., and Chun, C. H., 2003, "A Numerical Study of Turbulent Flow and Conjugate Heat Transfer in Concentric Annuli With Moving Inner Rod," Int. J. Heat Mass Transfer, **46**(19), pp. 3707–3716.
[14] Shigechi, T., and Lee, Y., 1991, "An Analysis on Fully Developed Laminar Fluid Flow and Heat Transfer in Concentric Annuli With Moving Cores," Int. J. Heat Mass Transfer, **34**(10), pp. 2593–2601.
[15] Kim, Y. J., 2000, "Unsteady MHD Convective Heat Transfer Past a Semi-Infinite Vertical Porous Moving Plate With Variable Suction," Int. J. Eng. Sci., **38**(8), pp. 833–845.
[16] Chamkha, A. J., 2004, "Unsteady MHD Convective Heat and Mass Transfer Past a Semi-Infinite Vertical Permeable Moving Plate With Heat Absorption," Int. J. Eng. Sci., **42**(2), pp. 217–230.
[17] Muralidhar, K., 1989, "Mixed Convection Flow in a Saturated Porous Annulus," Int. J. Heat Mass Transfer, **32**(5), pp. 881–888.
[18] Shigechi, T., Kawae, N., and Lee, Y., 1990, "Turbulent Fluid Flow and Heat Transfer in Concentric Annuli With Moving Cores," Int. J. Heat Mass Transfer, **33**(9), pp. 2029–2037.
[19] Lin, S., 1992, "Heat Transfer to Generalized Non-Newtonian Couette Flow in Annuli With Moving Outer Cylinder," Int. J. Heat Mass Transfer, **35**(11), pp. 3069–3075.
[20] Mozayyeni, H., and Rahimi, A. B., 2012, "Mixed Convection in Cylindrical Annulus With Rotating Outer Cylinder and Constant Magnetic Field With an Effect in the Radial Direction," Sci. Iran., **19**(1), pp. 91–105.
[21] Rahimi, A. B., and Abedini, A., 2013, "Numerical Study of Three-Dimensional Mixed Convection in an Eccentric Annulus," J. Thermophys. Heat Transfer, **27**(4), pp. 719–732.
[22] Malvandi, A., Moshizi, S., Soltani, E. G., and Ganji, D., 2014, "Modified Buongiorno's Model for Fully Developed Mixed Convection Flow of Nanofluids in a Vertical Annular Pipe," Comput. Fluids, **89**, pp. 124–132.
[23] Malvandi, A., and Ganji, D., 2015, "Effects of Nanoparticle Migration on Water/Alumina Nanofluid Flow Inside a Horizontal Annulus With a Moving Core," J. Mech., **31**(3), pp. 291–305.
[24] Shakiba, A., and Vahedi, K., 2016, "Numerical Analysis of Magnetic Field Effects on Hydro-Thermal Behavior of a Magnetic Nanofluid in a Double Pipe Heat Exchanger," J. Magn. Magn. Mater., **402**, pp. 131–142.
[25] Astanina, M. S., Riahi, M. K., Abu-Nada, E., and Sheremet, M. A., 2018, "Magnetohydrodynamic in Partially Heated Square Cavity With Variable Properties: Discrepancy in Experimental and Theoretical Conductivity Correlations," Int. J. Heat Mass Transfer, **116**, pp. 532–548.
[26] Jha, B. K., and Aina, B., 2015, "Mathematical Modelling and Exact Solution of Steady Fully Developed Mixed Convection Flow in a Vertical Micro-Porous-Annulus," Afrika Matematika, **26**(7–8), pp. 1199–1213.